ORIGINAL PAPER

The Influence of Small Hydrogen Admixtures up to 5 % to a Low Pressure Nonuniform Microwave Discharge in Nitrogen

J. Jovović · I. L. Epstein · N. Konjević · Yu A. Lebedev · N. M. Šišović · A. V. Tatarinov

Abstract We present the results of spectroscopic and 2D modeling study of the influence of hydrogen addition to non-uniform nitrogen plasma of electrode microwave discharge. The axial intensity distributions of the H_α line and N_2 (2^+: $C^3\Pi_u \to B^3\Pi_g$, 1^+: $B^3\Pi_g \to A^3\Sigma_u^+$) and N_2^+ (1^-: $B^2\Sigma_u^+ \to X^2\Sigma_g^+$) molecular bands are recorded for different incident microwave power input and hydrogen content. The corona model is used to determine electric field strength in nitrogen discharge from the intensity ratio of 2^+ and 1^- system of nitrogen bands. By means of 2D modeling spatial distributions of nitrogen molecules in $C^3\Pi_u$ state, microwave field strength, electron density, concentrations of N_2^+, N_4^+ are determined in nitrogen and in nitrogen–hydrogen mixtures. The concentration of N_2H^+ ions in nitrogen–hydrogen mixtures is determined also. The general conclusion of 2D modeling is in agreement with experimental results and shows that the influence of hydrogen addition to discharge is related to the fast conversion reactions of nitrogen ions (N_2^+, N_4^+) to N_2H^+ ion. These ion conversions lead to the change of ion plasma components transport properties, to the modification of microwave field strength in plasma, and consequently, to the alternation of all plasma parameters.

Keywords Non-uniform microwave nitrogen discharge · Hydrogen admixture · Optical emission spectroscopy · Nitrogen molecular ions · Self-consistent 2D modeling

Introduction

The extensive use of non-equilibrium plasma of electric discharges for solving various problems of plasma chemistry, light sources, and lasers requires development of methods of effective control over plasma parameters. Along with the choice of plasma gas and pressure, power and frequency of plasma maintaining electric field, gas admixtures, even
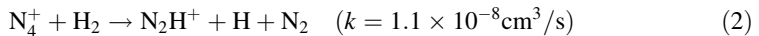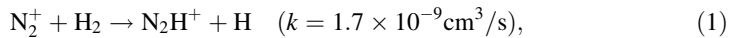
J. Jovović · N. Konjević (✉) · N. M. Šišović
Faculty of Physics, University of Belgrade, P.O. Box 368, Belgrade, Serbia
e-mail: nikruz@ff.bg.ac.rs

I. L. Epstein · Y. A. Lebedev · A. V. Tatarinov
Topchiev Institute of Petrochemical Synthesis, RAS, Leninsky Prospect 29, Moscow, Russia

when taken in small amounts (up to 5 %), are capable of strongly varying plasma properties. The influence of gas addition to self-sustained discharges is related mainly to the change of electric field strength, which is controlled by the balance of charged particles: the rate of ionization should be equal to the rate of charged particles loss. Several studies of the influence of gas addition to the change of ionization rate are described in [1–4]. Different admixtures with low potential of ionization were added to direct ionization conditions, while quenching admixtures were used to achieve stepwise ionization conditions, addition of CH_4 and N_2 to hydrogen plasma, etc. [1–4].

The explanation of the role of gas admixture to non-uniform discharges like e.g. electrode microwave discharges (EMD) is more complex in comparison with uniform discharge. As a result of inhomogeneity, the effect of gas additive in various regions of discharge is different. Moreover, the inhomogeneity of discharge produces new phenomena. One example is the influence of small amount (1–5 %) of Ar to the properties of EMD in nitrogen [5, 6]. The EMD is a representative of non-uniform discharges operating near the tip of microwave powered electrode/antenna in a discharge chamber of the size larger than characteristic plasma dimensions in the pressure range 0.5–400 Torr [7, 8].

This paper is devoted to the study of nitrogen EMD with hydrogen admixture. Earlier, preliminary results showed an increase of emission intensity of the second positive bands of nitrogen with an increase of hydrogen content in the external spherical part of the discharge and the effect was explained by ion conversion process [9]:

$$N_2^+ + H_2 \rightarrow N_2H^+ + H \quad (k = 1.7 \times 10^{-9} \text{cm}^3/\text{s}), \tag{1}$$

$$N_4^+ + H_2 \rightarrow N_2H^+ + H + N_2 \quad (k = 1.1 \times 10^{-8} \text{cm}^3/\text{s}) \tag{2}$$

where k is the rate constant.

This explanation was supported with results of simplified 1D model. It is known that consistency of modeling with experimental results depends on which plasma parameter is kept constant. Furthermore, 1D model does not correspond exactly to the experiments described in [9]. Namely, the experiments were performed with same incident microwave power whereas modeling was done with same microwave field strength at the electrode. The microwave field strength depends on the electrodynamics of the discharge and, with the same incident power, can vary with the change of plasma composition. Also, it is important to mention also that conclusions of [9] are based on spectroscopy measurements at two spatial points of the discharge. So, additional experimental and modeling study is required to confirm the effect of another gas addition described in [9].

In the case of non-uniform EMD plasma, the lower dimension, 1D model, can give results which are inconsistent with results of experiment, see e.g. [6]. The exact description of experiments and validation of conclusions presented in [9] can be done only on the base of higher dimension model (2D, 3D), which includes solution of Maxwell equations.

Recently, the results of 3D modeling of EMD in nitrogen and hydrogen were published [10]. It was shown that 3D model describes better structure of the microwave field in the chamber. This allows calculation of the characteristic sizes of the chamber to avoid the leakage of microwaves through the optical windows (the choice of the electrode/antenna length). The results of calculations of plasma properties in 3D and 2D models become the same if the leakage of microwaves through optical windows is much less than the incident power. In this case the wave disturbance caused by the window is absent and 3D geometry of the chamber is equivalent to 2D axially symmetric geometry. This condition corresponds to the experiments presented below. Moreover, 3D calculations require much more

computer resources than 2D calculations and, therefore, 2D model seems to be quite suitable for this study.

This paper presents results of spatially resolved spectroscopy study of the influence of hydrogen (1 and 5 %) added to nitrogen EMD. The experiment is supported by 2D modeling.

Experimental Setup and Model

Experimental Setup

The experimental set-up is shown schematically in Fig. 1. The magnetron (f = 2.45 GHz, P_{out} = 0–3 kW), driven with stabilized dc power supply (P_{out} = 0–5 kW), is used to generate plasma in cylindrical stainless steel chamber with an internal diameter of 82 mm and a length of 220 mm. The electrode with an external diameter of 12 mm was inserted 152 mm into the plasma chamber. Same electrode design was used in our preceding study of microwave induced plasma [11]. The only difference is the design of cylindrical copper antenna having conical truncated tip instead of a tungsten rod with a sharp conical ending [11]. The copper cylindrical tip has an external diameter of 5 mm and a length of 15 mm.
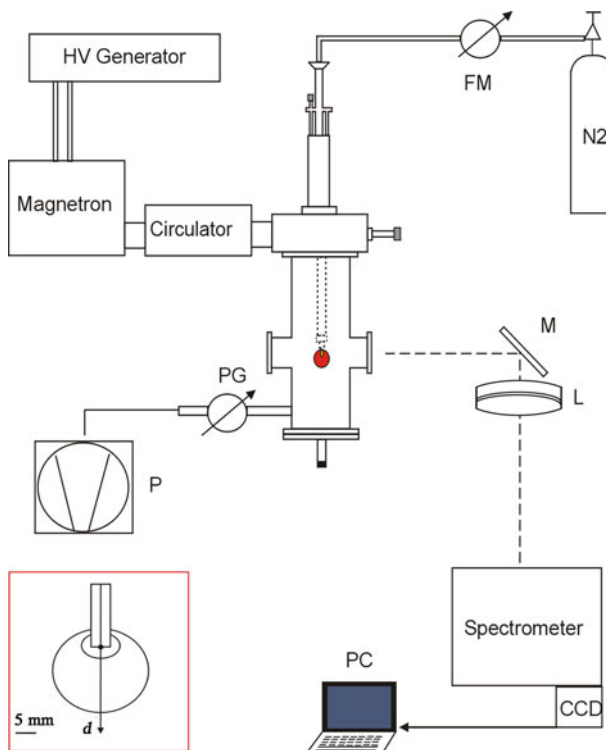

Fig. 1 The experimental setup: *PG* capacitive pressure gauge, *FM* volumetric flow controller, *M* mirror, *L* achromatic lens, *P* vacuum pump. The *inset* shows the position of coordinate d in respect to microwave discharge

The experiment is carried out in nitrogen (99.999 %) and nitrogen–hydrogen mixtures ($N_2 + 1$ % H_2, $N_2 + 5$ % H_2 vol.). The gas pressure in plasma chamber was measured with capacitive pressure gauge PG, see Fig. 1, and it was kept constant at 1 Torr for all experiments. The gas flow rate between 60 and 65 sccm was measured with volumetric flow controller (FM), see Fig. 1. The plasma was generated with incident microwave power of 125, 250 and 375 W. The reflected microwave power was measured indirectly by means of DC voltmeter connected to Schottky diode microwave coaxial detector mounted at the circulator port. The estimated ratio of reflected power over incident power was approximately 0.5.

Spectroscopic measurements of nitrogen molecular bands were performed with 2 m Ebert type spectrometer (inverse linear dispersion of 0.74 nm/mm in the first diffraction order with grating blazed at 500 nm). The discharge image was projected on the entrance slit of the spectrometer with unity magnification by means of a flat mirror M and an achromatic lens L (focal length 250 mm), see Fig. 1. Thermoelectrically cooled CCD ($2{,}048 \times 506$ pixels, pixel size 12×12 μm; -10 °C) was used as radiation detector. The axial distribution measurements were performed by moving lens along the vertical direction (coordinate d), in steps of 0.5 mm, see the inset in Fig. 1.

A standard coiled-coil tungsten halogen lamp was used for wavelength sensitivity calibration of the spectrometer-detector system.

Theoretical Model

For qualitative analysis of physico-chemical processes of the EMD in nitrogen and in nitrogen–hydrogen gas mixtures a self-consistent 2D model for nitrogen discharge [12] was used here as the basis for calculations.

The model includes Maxwell, Poisson and balance equations for charged and neutral species. Rate constants of processes with direct electron impact are assumed to be functions of the local value of the electric field and they are calculated using the electron energy distribution function (EEDF) obtained by solving time-independent homogeneous Boltzmann equation using two-term approximation. In order to calculate EEDF for nitrogen plasma by solving Boltzmann equation, it is necessary to take into account collisions of electrons with vibrationally excited nitrogen molecules (the super-elastic collisions). The effect of vibrationally excited nitrogen molecules to the plasma processes is accounted by using a simplified approach. The distribution function of nitrogen ground state molecules over the vibrational states or, so called, the vibrational distribution function (VDF), is described in the diffusion approximation and VDF is found self-consistent with EEDF. The applicability of this approach has been discussed in detail elsewhere [12].

The processes of the direct, stepwise and associative ionization, volume and wall recombination, ion conversion reactions and excitation and de-excitation processes are taken into account. The balance equations describe the kinetics of charged (e, N_2^+, N_4^+, H_2^+, N_2H^+) and neutral [$N_2(A^3\Sigma_u^+)$, $N_2(B^3\Pi_g)$, $N_2(C^3\Pi_u)$, $N_2(a'^1\Sigma_u^-)$, $N(^4S)$, $N(^2D)$, $N(^2P)$] plasma particles. It is shown in [12] that N_2^+ and N_4^+ are dominant ions under conditions typical for this work while relative concentrations of N^+, N_3^+ are considerably smaller. Thus, only ions N_2^+, N_4^+ and the reactions of their generation and loss are used for modeling of nitrogen plasma in the present study.

In the case of nitrogen–hydrogen mixture, nitrogen kinetic scheme was supplemented with reactions taken from [13] and for the description of hydrogen component we use a simplified approach described in [9].

At first this kinetic scheme was tested with 1D quasi-static code [9]. The analysis of Boltzmann equation for free plasma electrons has shown that for up to 5 % of hydrogen EEDF did not differ from EEDF in pure nitrogen. This simplification makes simulations easier and allows reliable interpretation of the influence of hydrogen on plasma parameters. The balance equations for neutral particles n_i are in the form:

$$-\bar{\nabla}.(D_i\bar{\nabla}_{n_i}) = S_i \tag{3}$$

and for charged particles n_j:

$$-\bar{\nabla}.(D_j\bar{\nabla}n_j + s\mu_j n_j\bar{\nabla}\phi) = S_j \tag{4}$$

Here D_i are the diffusion coefficients for all molecules and atoms, D_j and μ_j are free diffusion and mobility coefficients for electrons and positive ions, $S_{i/j}$ is the source term which defines the number of neutral/charged particles generated in unit volume per unit time, ϕ is a potential, $s = \pm1$ depending on the sign of charged particle. Here, we assume that diffusion coefficients are not functions of coordinates. The general form of the source term is given by:

$$S_{i/j} = \sum_m p_m\alpha k_m \prod_l n_l^\alpha \tag{5}$$

where $p_m = \pm1$ indicates production or loss of i/j particle in the m-th chemical reaction, k_m is the rate constant, n_l are concentrations of particles participating in this reaction and α is the stochiometric coefficient for each n_l.

In the simulation, we set the discharge pressure to 1 Torr, the percentage of the hydrogen additive was 1 and 5 %, the gas temperature 300 K and the incident power 30 W. The geometry and dimensions of the discharge chamber in simulations coincide with those described in "Experimental Setup" section. All simulations were carried out using a commercially available package COMSOL (v. 3.5a) [14]. The simulation mesh size is chosen to be close to the spatial resolution of the experiment ($\sim$0.3 mm).

Special comments should be given about the choice of incident power in our calculation. As pointed out in "Experimental Setup" section, the incident microwave power was up to several hundreds Watts and the estimated absorbed power by plasma was an half of the incident power. It is well known that different channels of energy loss exist in the microwave transmission line between the power meter and plasma and, thus, the real plasma absorbed power is small, (7–10) % of incident power [15]. It is also known that the external diameter of EMD depends on plasma absorbed power: the higher absorbed power, the larger is plasma diameter [7, 8], see also "Experimental Results" section. Since all power loss channels can't be taken into account in our model, the coincidence of calculated and measured discharge diameters is used as a criterion of correctness of assumed 30 W of plasma absorbed power in modeling. The value of discharge diameter obtained by modeling at absorbed power of 30 W corresponds well to measured plasma diameter.

Results and Discussion

Experimental Results

The axial intensity distributions of spectral lines or bands belonging to various species, see Table 1, recorded from 1 Torr nitrogen EMD operated with different incident microwave

Table 1 Wavelength and transitions of the observed spectral lines and bands

Excited species	Transition	Peak wavelength (nm)
H	Hα $(3 \rightarrow 2)$	656.3
N_2	$C^3\Pi_u \rightarrow B^3\Pi_g$	337.0
N_2	$B^3\Pi_g \rightarrow A^3\Sigma_u^+$	662.4
N_2^+	$B^2\Sigma_u^+ \rightarrow X^2\Sigma_g^+$	391.4

power and different content of hydrogen are presented in Figs. 2, 3, 4, 5, 6. It is evident that emission intensities of all molecular bands and the H_α line increase with incident power. The discharge size is estimated from the spatial intensity distribution as a contour in the spherical part of discharge where it changes from "plateau" region to decay region. This change is best pronounced within spatial distributions of second positive $(2^+:$ $C^3\Pi_u \rightarrow B^3\Pi_g)$ and first positive $(1^+: B^3\Pi_g \rightarrow A^3\Sigma_u^+)$ band intensity. It is seen also that the external discharge dimension increases with the incident power.
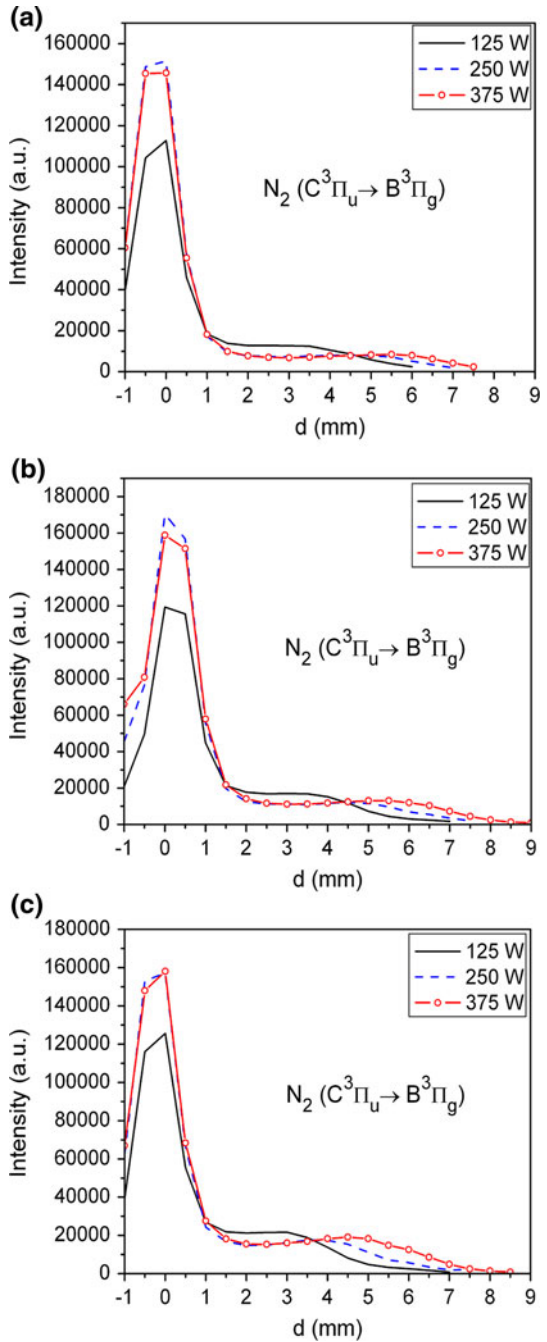
The influence of hydrogen admixture may be understood from Fig. 6. The addition of hydrogen apparently decreases the intensity of first negative $(1^-: B^2\Sigma_u^+ \rightarrow X^2\Sigma_g^+)$ nitrogen ion band emission for 25 % in the near electrode region and for 90 % in the central part of plasma. The emission of 1^+ nitrogen band is only slightly decreased in both regions of discharge, see Fig. 6c. The dimension of EMD is also decreasing function of hydrogen concentration. The influence of hydrogen on 2^+ band emission is more complex, see Fig. 6, where one can see non-monotonous change of intensity in the near electrode region and increase of intensity with addition of hydrogen in the periphery of discharge.

By applying the corona model approximation from relative intensities of 2^+ system of nitrogen and 1^- system of N_2^+ band, the measurement of microwave electric field in the near electrode region of EMD can be performed. The corona model applicability to the near electrode region of EMD is described in detail elsewhere [16]. In this region of EMD, an electron impact is the main channel of heavy particles excitation, while the radiative decay represents main channel for deactivation of excited particles. The intensities of 337.0 nm $(2^+$ system) and 391.4 nm $(1^-$ system) bands are used for corona model calculations. The method is based on comparison of measured ratio of intensities of these two bands with the ratio calculated from the Boltzmann equation by varying electric field strength. The equality of ratios is reached for the value of the field strength that corresponds to experimental condition. This method gives the electric field averaged along a line of sight: 390 V/cm (125 W), 480 V/cm (250 W), 530 V/cm (375 W). As the radial distribution of emission intensity is non-uniform and microwave field in near electrode region is 4–5 times larger than in other parts of EMD, the measured field corresponds to the region near the electrode tip. Unfortunately, this method can't be used in the mixture of nitrogen with hydrogen since nitrogen ion concentration is strongly controlled by the ion conversion in collisions with hydrogen molecules.
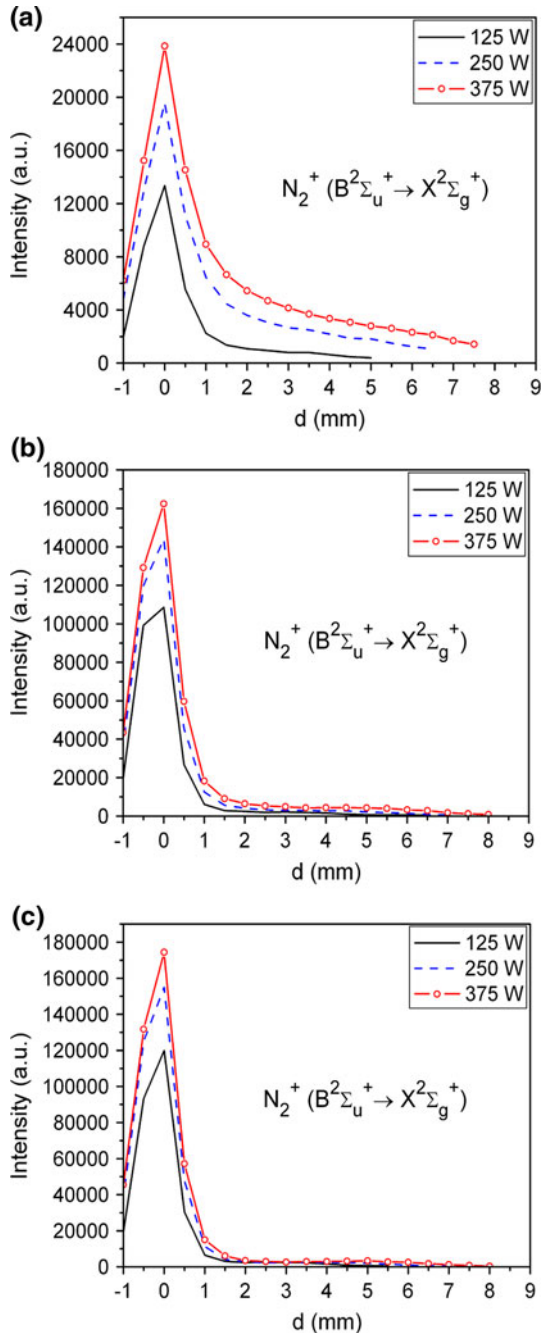
Results of 2D Modeling

The results of modeling are shown in Figs. 7, 8, 9, 10, 11, 12, 13, 14. The 2D diagrams of microwave field spatial distribution together with the concentration distribution of molecules in $C^3\Pi_u$-state are given in Fig. 7. The diagrams of microwave electric field and concentration of nitrogen molecules in $C^3\Pi_u$-state are presented for pure nitrogen only since it is very difficult to visualize changes of given plasma parameters in

Fig. 2 Measured axial distributions of the intensity of second positive $[N_2(C^3\Pi_u \rightarrow B^3\Pi_g)]$ band (337.0 nm) of nitrogen at different incident powers in **a** pure nitrogen, **b** $N_2 + 1\% H_2$, and **c** $N_2 + 5\% H_2$


nitrogen–hydrogen mixtures. The influence of hydrogen on parameters of nitrogen EMD is more pronounced in 2D diagrams of N_4^+ concentration in Fig. 8 and electron density in Fig. 9 as well as in axial distributions of plasma parameters, see Figs. 10, 11, 12, 13, 14.

Fig. 3 Measured axial intensity distributions of the first negative $[N_2^+(B^2\Sigma_u^+ \to X^2\Sigma_g^+)]$ band (391.4 nm) of nitrogen ion at different incident powers in **a** pure nitrogen, **b** $N_2 + 1\% H_2$, and **c** $N_2 + 5\% H_2$


Before comparing results of experiments and modeling a few comments should be given. The reported axial distributions of plasma emission intensity represent an averaged value along the line-of-sight whereas results of modeling, Figs. 10, 11, 12, 13, 14, are the axial distributions of emitting particles, which are proportional to the emission intensity.

Fig. 4 Measured axial intensity distributions of the first positive [$N_2(B^3\Pi_g \rightarrow A^3\Sigma_u^+)$] band (662.4 nm) of nitrogen at different incident powers in **a** pure nitrogen, **b** $N_2 + 1\% H_2$, and **c** $N_2 + 5\% H_2$
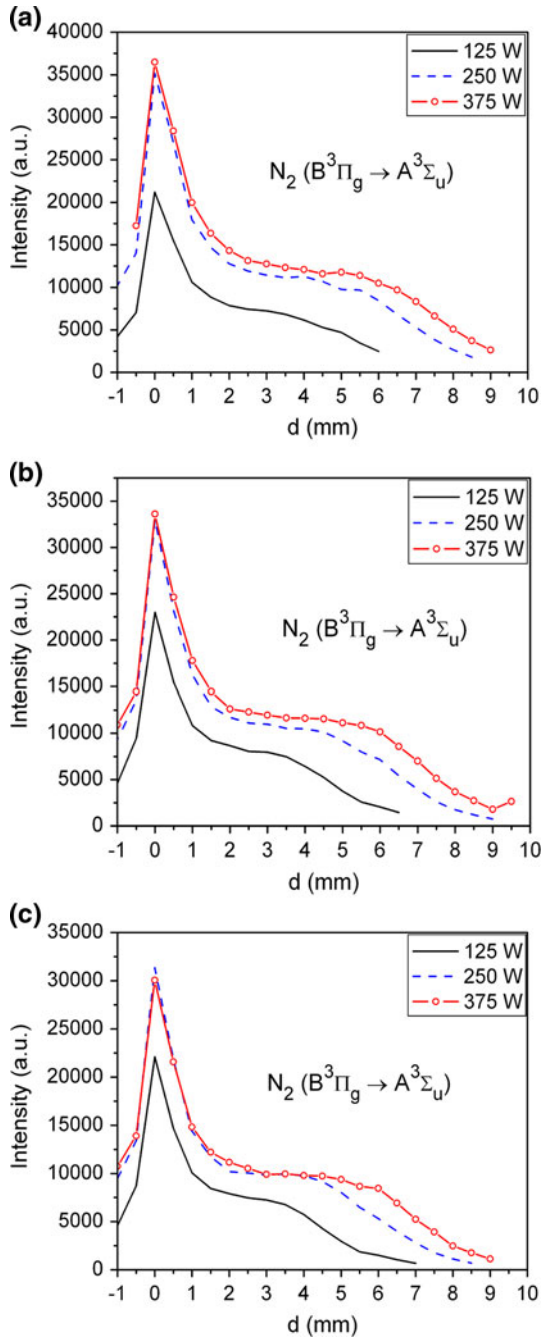
This difference between experiment and modeling data would be compensated by Abel transformation of modeling results, if the experimental data may be Abel transformed as well. This was not possible in a present setup since we used a lens that focuses the plane of

Fig. 5 Measured axial intensity distributions of the H_α at different incident powers in **a** $N_2 + 1\%$ H_2 and **b** $N_2 + 5\%$ H_2
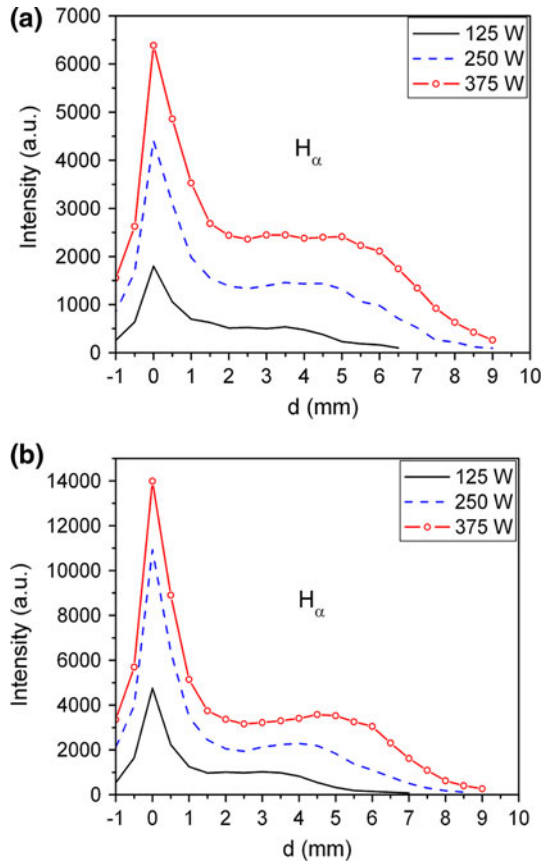

discharge region near the axis of the electrode to the slit of monochromator, see Fig. 1. In this case results of measurements are also averaged along the line-of-sight, but the "weight" of emissivity from different points of the discharge will be different depending on the resolution depth of the optical system. The emission from axial region gives maximal contribution to registered optical signal. Therefore, the experimental results can be attributed mainly to the central part of discharge. Hence, there is no need in using the Abel transformation of model data.

The results of 2D modeling, presented in Figs. 10, 11, 12, 13, 14 are in qualitative agreement with experimental results. Namely, Fig. 10 shows that the concentration of nitrogen molecules in $C^3\Pi_u$ state, responsible for 2^+ bands emission, increases at the discharge periphery (spherical part) with addition of hydrogen (compare with Fig. 6). The change in near electrode region resembles the experiment and shows non-monotonous dependence on hydrogen concentration. The calculated discharge dimension is close to one determined from spectroscopy data.

It is necessary to outline that microwave field strength, estimated from measured emission spectra (see above) and averaged over the near electrode region differs 10–30 % from modeled values, see Fig. 11. This gives an additional validation for the choice of small absorbed microwave power as an initial modeling parameter, what is already pointed out in "Experimental Results" section. The Fig. 11 shows that, in contrast to 1D model,

Fig. 6 Measured axial intensity distributions of **a** the second positive band, **b** first negative band and **c** first positive band of nitrogen at incident power 250 W in nitrogen, $N_2 + 1$ % H_2 and $N_2 + 5$ % H_2
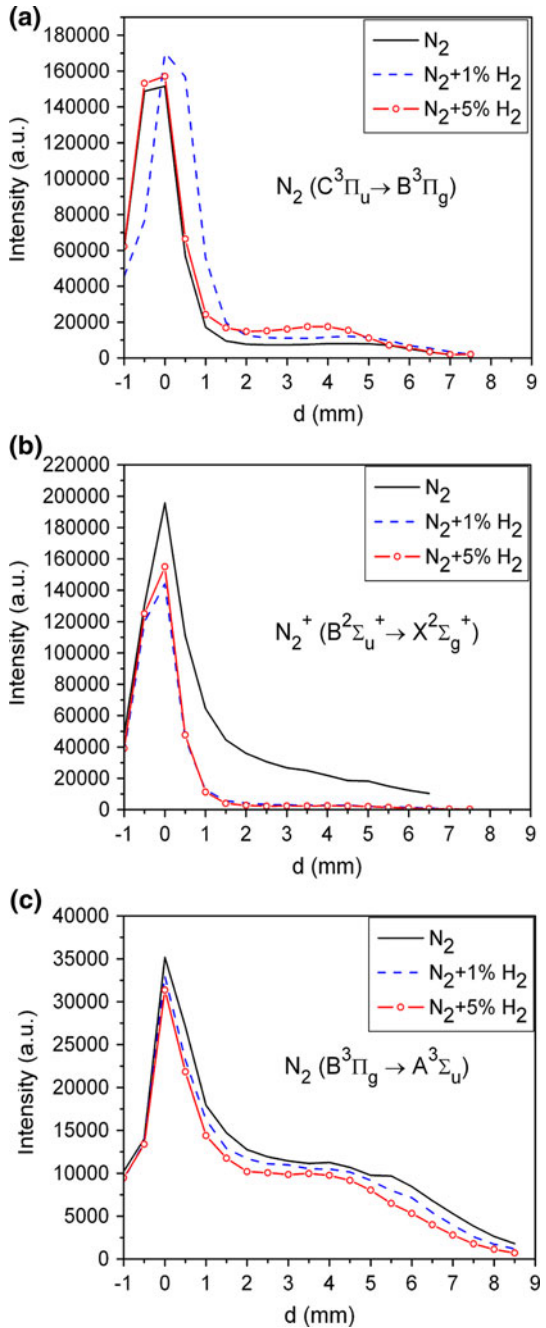
electric field strength at the electrode tip depends on hydrogen concentration. The decrease of electric field strength in the near electrode region is accompanied with an increase of electric field strength at the discharge periphery, which is result of the increase of hydrogen concentration. The calculations also show that maximum of electric field strength in the
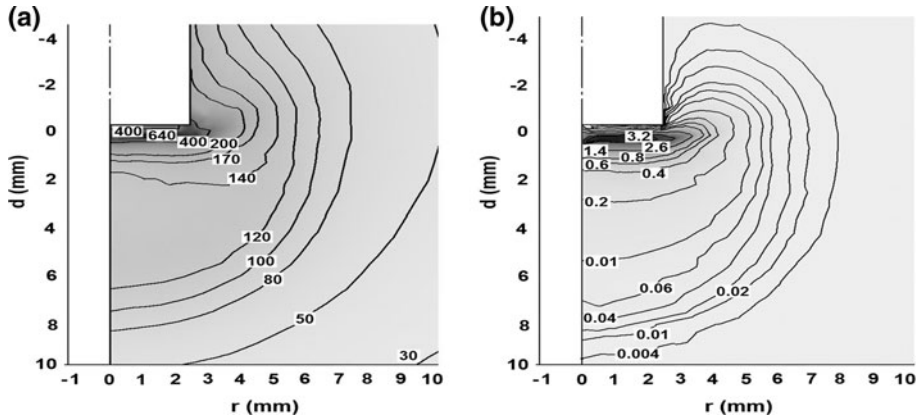
Fig. 7 Calculated spatial distributions of **a** microwave electric field and **b** concentration of nitrogen molecules in C$^3\Pi_u$-state, normalized to critical electron density $n_c \approx 7 \times 10^{10}$ cm^{-3}, in pure nitrogen EMD

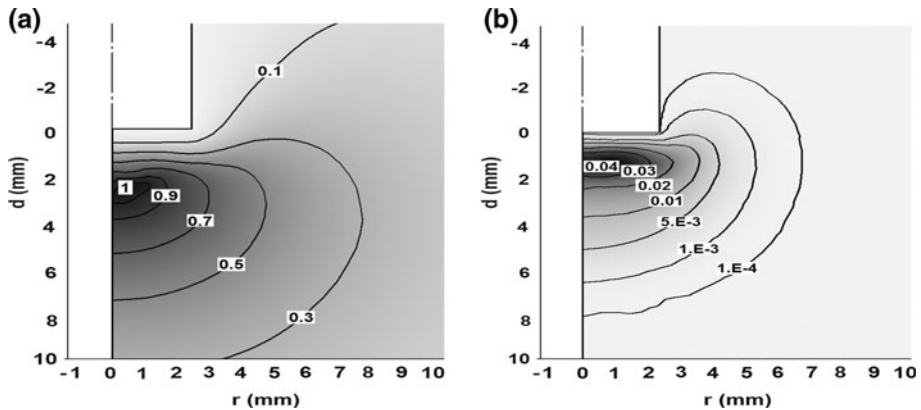**Fig. 8** Calculated spatial distributions of N$_4^+$ ion concentration in EMD in **a** pure nitrogen and in **b** N$_2$ + 5 % H$_2$. Concentrations of N$_4^+$ ions are normalized to critical electron density $n_c \approx 7 \times 10^{10}$ cm^{-3}

near electrode region decreases and moves away axially from the electrode tip. Hence, small addition of hydrogen increases a thickness of the near electrode region.

Furthermore, the addition of hydrogen decreases electron density in EMD, see Figs. 9 and 12. The concentration of N$_2^+$ ion significantly decreases, which is more pronounced in the spherical part of EMD (compare Figs. 13 and 6b). With addition of hydrogen maxima of N$_2^+$ and N$_4^+$ concentrations, see Figs. 8 and 13, move towards the electrode in axial direction. At hydrogen concentration of 5 %, concentration of N$_4^+$ is very small. Changes of N$_2$H$^+$ concentration are shown in Fig. 14.

The influence of small addition of hydrogen (up to 0.5 percent by volume) on characteristics of quasi homogeneous non-equilibrium plasma of DC discharge was studied previously, see e.g. [17, 18]. The addition of hydrogen always increases the intensity of 2$^+$ bands emission of nitrogen. In [17], this effect is related to an increase of vibrational relaxation of ground state nitrogen molecules in collisions with hydrogen molecules, which

Fig. 9 Calculated spatial
distributions of the electron
density in EMD in pure nitrogen
(*solid lines*) and in $N_2 + 5 \% H_2$
(*dashed lines*). Values of electron
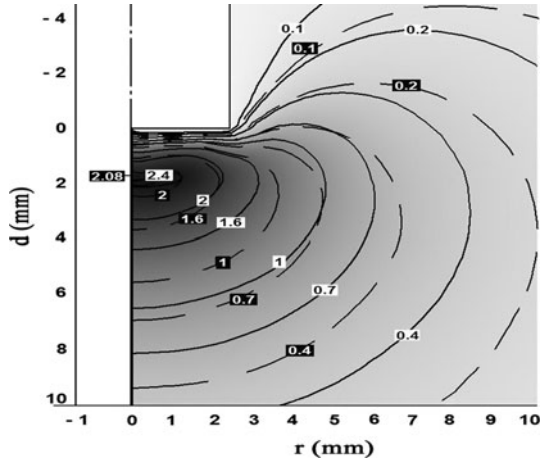density are normalized to
$n_c \approx 7 \times 10^{10}$ cm^{-3}

Fig. 10 Theoretical axial
profiles of $N_2(C^3\Pi_u)$ molecules
in (*1*) pure nitrogen, (*2*)
$N_2 + 1 \% H_2$ and (*3*)
$N_2 + 5 \% H_2$ determined by 2D
modeling. Concentrations are
normalized to the critical plasma
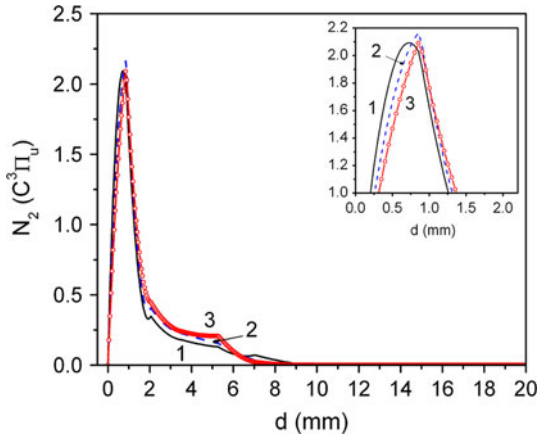electron density n_c
($n_c \approx 7 \times 10^{10}$ cm^{-3})

Fig. 11 Theoretical axial
profiles of electric field strength
in (*1*) nitrogen, (*2*) $N_2 + 1 \% H_2$,
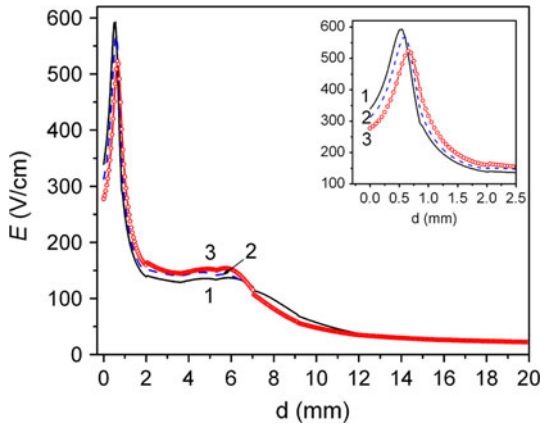and (*3*) $N_2 + 5 \% H_2$ evaluated
by 2D modeling

Fig. 12 Theoretical axial profiles of electron density in (*1*) nitrogen, (*2*) N_2 + 1 %H_2 and (*3*) N_2 + 5 %H_2 after 2D modeling. Concentrations are normalized to the critical plasma electron density n_c ($n_c \approx 7 \times 10^{10}$ cm^{-3})
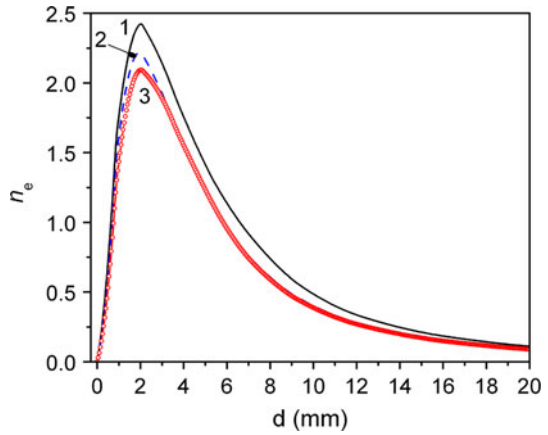

Fig. 13 Theoretical axial profiles of N_2^+ (*solids*) and N_4^+ (*dashed*) in (*1*) nitrogen, (*2*) N_2 + 1 %H_2 and (*3*) N_2 + 5 %H_2 obtained by 2D modeling. Concentrations are normalized to the critical plasma electron density n_c ($n_c \approx 7 \times 10^{10}$ cm^{-3})

Fig. 14 Theoretical axial profiles of N_2H^+ in (*2*) N_2 + 1 %H_2 and (*3*) N_2 + 5 %H_2 obtained by 2D modeling. Concentrations are normalized to the critical plasma electron density n_c ($n_c \approx 7 \times 10^{10}$ cm^{-3})
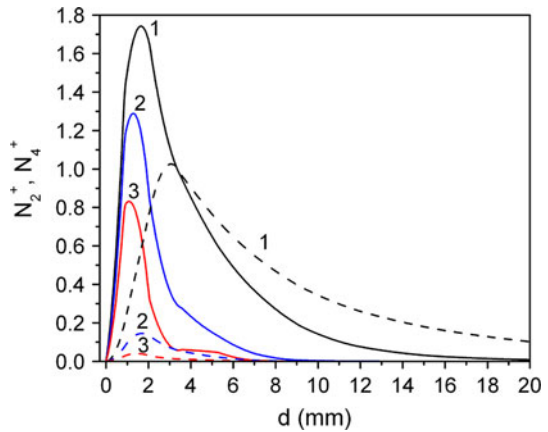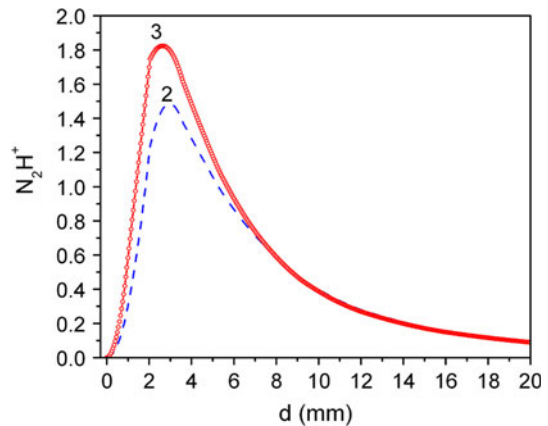
decrease concentration of vibrationally excited nitrogen molecules involved in ionization. This process leads to an increase of the reduced electric field required to maintain concentration of N_2 molecules. In accordance with [18], the addition of hydrogen changes ionization mechanism from stepwise to direct electron impact ionization, which in general requires higher reduced electric field. The change of reduced electric field strength is controlled by a balance of charged particles and is related with ionization process in both cases [17, 18]. In [17, 18], ion conversion was not considered as a possible mechanism which changes plasma properties. The comparison of these results with EMD experimental data indicates that the situation is more complex in a non-uniform discharge and that the effect of gas addition is space dependent as well.

The experimental study of an influence of hydrogen admixture in nitrogen EMD and 2D modeling confirmed conclusion of [9] on the key role of high rate ion conversion reactions to properties of strongly non-uniform discharge, see Introduction. The coincidence of general conclusion from 1D and 2D modeling could not be predicted *a priory* for non-uniform plasma. The results from [7] showed different conclusions from these two models for Ar admixture to nitrogen plasma. The change of ion composition causes variation of transport properties of ionic component. This is especially obvious in case of significant change of the ion mass which is result of ion conversion. It is known that principal ion in the electrode region of EMD is N_2^+ ion while in the spherical region it is N_4^+. In case of hydrogen addition, the principal ion in entire discharge is N_2H^+. Therefore, the replacement of heavy ion by lighter one in the spherical region increases the rate of its loss and lead to an increase of electric field strength. So in this case, contrary to [17, 18], the increase of the field strength is caused by the change of charge particles loss. It should be also noted that in the case of microwave nitrogen plasma at pressures below several Torrs and field frequency 2.45 GHz, the EEDF depends on E/ω instead of E/N and the electric field does not depend on gas temperature [19].

Summary and Conclusions

Optical emission spectroscopy with good spatial resolution and 2D modeling provided comprehensive information about the influence of hydrogen addition to non-uniform, low pressure nitrogen EMD plasma. It is shown that the addition of hydrogen changes plasma properties: (1) the intensity of first negative band of nitrogen ion emission decreases with addition of hydrogen; the decrease is more pronounced in the spherical part of EMD, while the emission of negative ion in the mixture is concentrated in near electrode region only; (2) the emission of first positive nitrogen band only slightly decreases; (3) with addition of hydrogen the second positive band shows non-monotonous change of intensity in the near electrode region and an increase of intensity in the periphery of the discharge; (4) the microwave field in near electrode region decreases (maximum of electric field moves away from the electrode along the axis and the thickness of near electrode region increases) and this is accompanied with an increase of electric field in the discharge periphery; (5) the electron density decreases with hydrogen addition, but maximum of the concentration is always above critical value; (6) concentrations of N_2^+ and N_4^+ ions strongly decrease with hydrogen and maximum of concentrations move towards the electrode, the concentration of N_4^+ becomes negligible at hydrogen concentrations of 5 %; (7) the concentration of N_2H^+ increases and, for 5 % of hydrogen, this ion becomes the principal one at the periphery of discharge with comparable concentration to N_2^+ in the near electrode region. The dimension of EMD is decreasing function of hydrogen concentration.

The results of 2D modeling shows that, in spite of numerous differences in the description of plasma properties by 1D modeling [9], the general conclusion about the influence of hydrogen to nitrogen strongly non-uniform microwave discharge is not changed essentially: the fast conversion reactions of nitrogen ions (N_2^+, N_4^+) into N_2H^+ ion are responsible for alterations of plasma properties caused by the change of charge particles loss in the balance equation for charged particles.

References

 1. Fortov VE (ed) (2000) Encyclopedia of low temperature plasma, introductory, vol 3, chap 8. Nauka, Moscow
 2. Gomes-Aleixandre C, Sanches O, Castro A, Albella JM (1993) J Appl Phys 74:3752–3757
 3. Bardos L, Barankova H, Lebedev YA, Nyberg T, Berg S (1997) Diam Relat Mater 6:224–229
 4. Asmussen J, Gu Y, Lu J (2011) Proceedings of 8th international workshop "strong microwaves and terahertz waves: sources and applications", Nizhny Novgorod, Russia, vol 5, pp 5–6
 5. Lebedev Y, Mavlyudov T, Epstein I, Chvyreva A (2010) Contributed papers of 25th symposium on the physics of ionized gases, Donji Milanovac, Serbia, pp 253–256
 6. Lebedev Y, Mavlyudov T, Epstein I, Tatarinov A, Chvyreva A (2012) Plasma Sour Sci Technol 21:015015–015025
 7. Lebedev YA, Mokeev MV, Solomakhin PV, Shakhatov VA, Epstein IL (2008) J Phys D Appl Phys 41:194001–194004
 8. Lebedev YA, Epstein IL, Tatarinov AV, Shakhatov VA (2010) J Phys, Conf Ser 207:012002–012011
 9. Lebedev YA, Mavlyudov TB, Shakhatov VA, Epstein IL (2010) High Temp 48:315–320
10. Lebedev YuA, Tatarinov AV, Epstein I (2011) L. High Temp 49:775–787
11. Jovović J, Šišović NM, Konjević N (2010) Vaccum 85:187–192
12. Lebedev YA, Tatarinov AV, Epstein IL (2007) Plasma Sour Sci Technol 16:726–733
13. Tatarova E, Dias FM, Gordiets B, Ferreira CM (2005) Plasma Sour Sci Technol 14:19–31
14. COMSOL 3.5a. http://www.comsol.com/
15. Lebedev YA, Mokeev MV (2001) Plasma Phys Rep 27:418–423
16. Lebedev YA, Solomakhin PV, Shakhatov VA (2008) Plasma Phys Rep 34:562–573
17. Golubovskii YB, Telezhko VM (1984) Zh Tekh Fiz (in Russian) 54:1262–1268
18. Popa SD, Hochard L, Ricard A (1997) J Phys III France 7:1331–1337
19. Lebedev YA (1998) J Phys IV France 8:Pr7-369–Pr7-380